

## LETTERS

# An unconventional myosin in *Drosophila* reverses the default handedness in visceral organs

Shunya Hozumi<sup>1</sup>, Reo Maeda<sup>1</sup>, Kiichiro Taniguchi<sup>1</sup>, Maiko Kanai<sup>1</sup>, Syuichi Shirakabe<sup>1</sup>, Takeshi Sasamura<sup>1</sup>, Pauline Spéder<sup>3</sup>, Stéphane Noselli<sup>3</sup>, Toshiro Aigaki<sup>4</sup>, Ryutaro Murakami<sup>5</sup> & Kenji Matsuno<sup>1,2</sup>

The internal organs of animals often have left–right asymmetry<sup>1,2</sup>. Although the formation of the anterior–posterior and dorsal–ventral axes in *Drosophila* is well understood, left–right asymmetry has not been extensively studied. Here we find that the handedness of the embryonic gut and the adult gut and testes is reversed (not randomized) in viable and fertile homozygous *Myo31DF* mutants. *Myo31DF* encodes an unconventional myosin, *Drosophila* MyoIA (also referred to as MyoID in mammals; refs 3, 4), and is the first actin-based motor protein to be implicated in left–right patterning. We find that *Myo31DF* is required in the hindgut epithelium for normal embryonic handedness. Disruption of actin filaments in the hindgut epithelium randomizes the handedness of the embryonic gut, suggesting that *Myo31DF* function requires the actin cytoskeleton. Consistent with this, we find that *Myo31DF* colocalizes with the cytoskeleton. Overexpression of *Myo61E*, another myosin I (ref. 4), reverses the handedness of the embryonic gut, and its knockdown also causes a left–right patterning defect. These two unconventional myosin I proteins may have antagonistic functions in left–right patterning. We suggest that the actin cytoskeleton and myosin I proteins may be crucial for generating left–right asymmetry in invertebrates.

Mechanisms that create characteristic left–right asymmetry have been studied extensively in vertebrates<sup>2</sup>. However, although the organs of many invertebrate species also have left–right asymmetry, the mechanisms by which this asymmetry arises are largely unknown. In *Drosophila*, several organs have left–right asymmetry, including the embryonic gut, the adult brain and the genitalia<sup>5–9</sup>.

To identify genes involved in left–right asymmetry of the *Drosophila* embryonic gut, we performed a genetic screen using a collection of P-element lines (Gene Search, <http://gsdb.biol.metro-u.ac.jp/%7Edclust/>). The embryonic gut is composed of three major parts, the foregut, midgut and hindgut, all of which have characteristic left–right asymmetry<sup>5</sup> (Fig. 1c, e, h and Table 1, row 1). We found that 75.7% of homozygous *Myo31DF<sup>souther</sup>* embryos show synchronous inversion of the midgut and hindgut (Fig. 1d, f and Table 1, row 2). In these embryos, the hindgut and midgut are the mirror-image of those in wild-type embryos, rather than showing randomized patterning (binominal test,  $P \leq 0.01$ ). In contrast, foregut handedness was normal in all cases examined, indicating that this phenotype was heterotaxial (Fig. 1i and Table 1, row 2). *Myo31DF<sup>souther</sup>* is a background mutation of the Gene Search *Drosophila* line GS14508. We used deficiency mapping to map the cytological location of *Myo31DF<sup>souther</sup>* to between 30D and 31F (data not shown). We then performed complementation tests between *Myo31DF<sup>souther</sup>* and lines bearing mutations that map to this region. *Myo31DF<sup>souther</sup>*

failed to complement *Myo31DF<sup>K1</sup>* (described in ref. 10), an allele of *Myo31DF* encoding *Drosophila* MyoID<sup>3,4</sup>.

The transposable element *gypsy* was inserted into the 5′-untranslated region of the *Myo31DF* gene in *Myo31DF<sup>souther</sup>* (Fig. 1a). *Myo31DF<sup>L152</sup>* was one of five ethylmethanesulfonate (EMS)-induced *Myo31DF* alleles isolated in a large-scale EMS mutant screen (details of the screen will be presented elsewhere). *Myo31DF<sup>L152</sup>* has a base substitution that introduces a premature stop codon at amino acid 331, resulting in a putative truncated product (Fig. 1a). *Myo31DF* overexpression from *UAS-Myo31DF* driven by *byn-Gal4* in the hindgut and posterior midgut and their primordial counterparts rescued the left–right defects of *Myo31DF<sup>souther</sup>* embryos (Supplementary Table 1, row 22)<sup>11</sup>, indicating that *Myo31DF* was responsible for the heterotaxia. In *Myo31DF<sup>souther</sup>* embryos, NP2432-driven expression of *Myo31DF* in the hindgut epithelium (Table 1, row 12), but not in other parts of the embryonic gut, such as the midgut and mesoderm (Supplementary Table 1, rows 24 and 25), was sufficient to rescue this heterotaxia, suggesting that *Myo31DF* is required in the hindgut epithelium. Furthermore, the frequency of the handedness defect was similar in *Myo31DF<sup>L152</sup>* homozygous and *Myo31DF<sup>L152</sup>/Df(2L)J2* embryos (Table 1, rows 3 and 4; see Methods). Thus, *Myo31DF<sup>L152</sup>* is probably a null mutant of *Myo31DF*. All homozygous *Myo31DF* mutants isolated in this study were viable and fertile, with normal hindgut tissue specification, suggesting that *Myo31DF* function is largely restricted to left–right patterning (data not shown). We did not detect a maternal phenotype or *Myo31DF* gene contribution ( $0.2 < P < 0.3$ ,  $\chi^2$  test; Supplementary Table 1, rows 5 and 6). Notably, the foregut became a mirror-image of its wild-type counterpart when *Myo31DF* was overexpressed in the entire embryo, but other parts of the gut were normal<sup>12</sup> (Fig. 1j and Supplementary Table 1, row 7). Therefore, we suggest that *Myo31DF* is not involved in the left–right asymmetrical development of the foregut in wild-type embryos, but can reverse foregut handedness.

We next examined the adult hindgut and testes, which are regenerated during metamorphosis. These also showed inverted handedness in the *Myo31DF* homozygote (Fig. 1l, n, p and Table 1, rows 2 and 3). In most *Myo31DF<sup>L152</sup>* adults, the loop of the hindgut and spiral of the testes were reversed (binominal test,  $P \leq 0.01$ ), although not always synchronously (Table 1, row 3). We then knocked-down the function of the *Myo31DF* gene using RNA interference (RNAi) *in vivo*. The expression of double-stranded *Myo31DF* RNA driven by *byn-Gal4* caused inversion of the adult, but not the embryonic, hindgut (Supplementary Table 1, row 9). Thus, the left–right pattern involving *Myo31DF* is not transmitted during metamorphosis.

<sup>1</sup>Department of Biological Science and Technology, and <sup>2</sup>Genome and Drug Research Center, Tokyo University of Science, 2641 Yamazaki, Noda, Chiba 278-8510, Japan.

<sup>3</sup>Institute of Signalling, Developmental Biology & Cancer, UMR6543-CNRS, University of Nice Sophia-Antipolis, Parc Valrose, 06108 Nice Cedex 2, France. <sup>4</sup>Department of

Biological Science, Tokyo Metropolitan University, 1-1 Minami-osawa, Hachioji, Tokyo 192-0397, Japan. <sup>5</sup>Department of Physics, Biology, and Informatics, Yamaguchi University, 1677-1 Yoshida, Yamaguchi, Yamaguchi 753-8512, Japan.

*In situ* hybridization revealed *Myo31DF* expression in the amnioproctodeal invagination at stage 6 (Fig. 2a). At stages 12–14, *Myo31DF* messenger RNA was strongly detected in the primordial midgut and hindgut (Fig. 2b), and in the proventriculus, midgut and

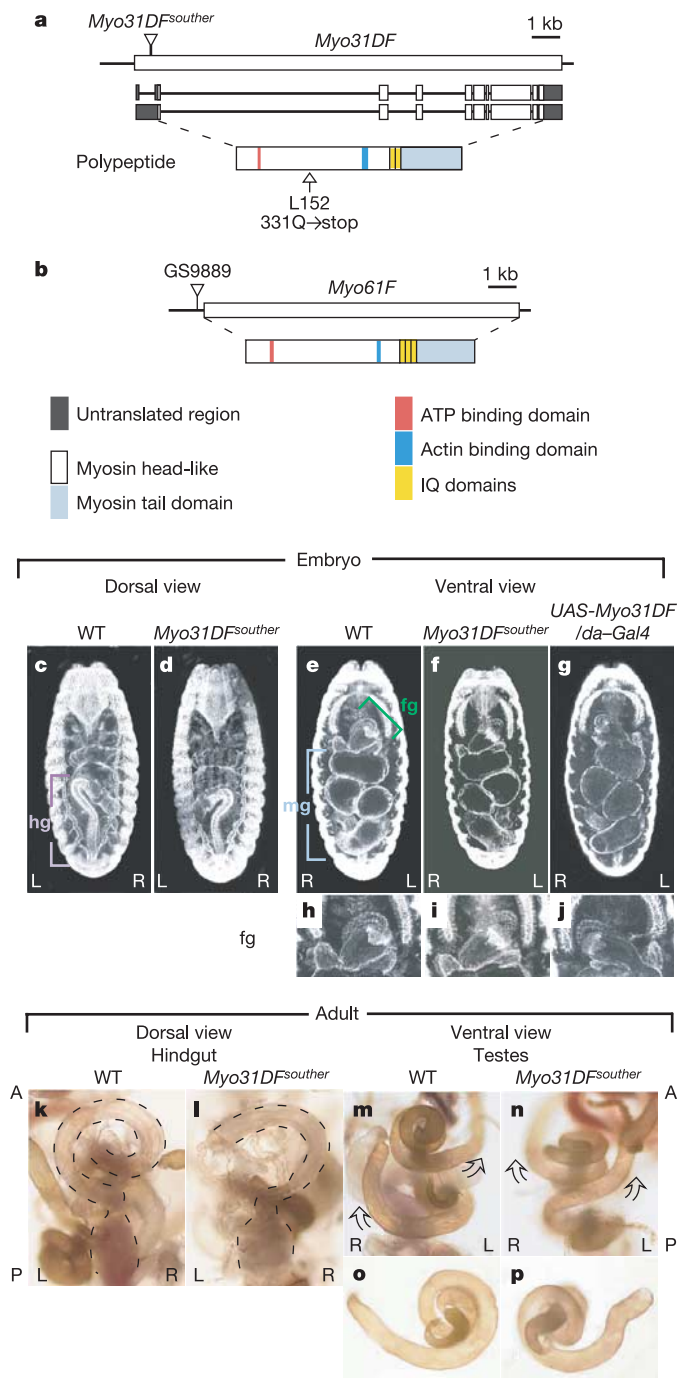


**Figure 1 | *Myo31DF* mutation inverses the handedness of embryonic and adult visceral organs.** **a**, Schematic of molecular lesions in *Myo31DF*<sup>L152</sup> and *Myo31DF*<sup>souther</sup>. **b**, In the GS9889 line, a GS vector is inserted upstream of the *Myo61F* locus. Motifs in *Myo31DF* and *Myo61F* are shown. **c, e**, Wild-type embryos. **d, f**, *Myo31DF*<sup>souther</sup> embryos. **g**, Embryo overexpressing *Myo31DF* driven by *da-GAL4*. **h–j**, Higher-magnification views of the foregut images shown in **e–g**. **k**, Wild-type adult hindgut. **l**, *Myo31DF*<sup>souther</sup> adult hindgut. **m**, Wild-type adult with testes located anteriorly and posteriorly, elongating to the left and right, respectively. **n**, *Myo31DF*<sup>souther</sup> adult, showing mirror-image handedness of testes. **o, p**, Testes viewed from the ejaculatory duct in wild-type (**o**) and *Myo31DF*<sup>souther</sup> (**p**) adults. Abbreviations: fg, foregut; hg, hindgut; mg, midgut; L, left; R, right; A, anterior; P, posterior.

hindgut (Fig. 2c). A sense-strand probe of *Myo31DF* gave no detectable signal (Fig. 2d). Immunostaining of wild-type embryos with an anti-Myo31DF antibody (anti-Myo31DF-1P) also labelled the midgut and hindgut (Fig. 2e–g). These signals were absent in *Myo31DF*<sup>souther</sup> and *Myo31DF*<sup>L152</sup> homozygotes, indicating that the staining was specific (Fig. 2h and data not shown). *Myo31DF* mRNA and protein were detected in a symmetrical pattern before the development of left–right asymmetry (data not shown). *Myo31DF* protein is expressed in the adult gut<sup>4</sup>. We did not detect *Myo31DF* expression in the foregut, which may account for the absence of any laterality defect in the foregut of *Myo31DF* mutants.

*Myo31DF* protein binds to actin in an ATP-dependent manner<sup>4</sup>. We next examined the co-localization of *Myo31DF* and the actin cytoskeleton in cultured *Drosophila* S2 cells. A green fluorescent protein (GFP)-tagged *Myo31DF* (*Myo31DF*-GFP) had wild-type

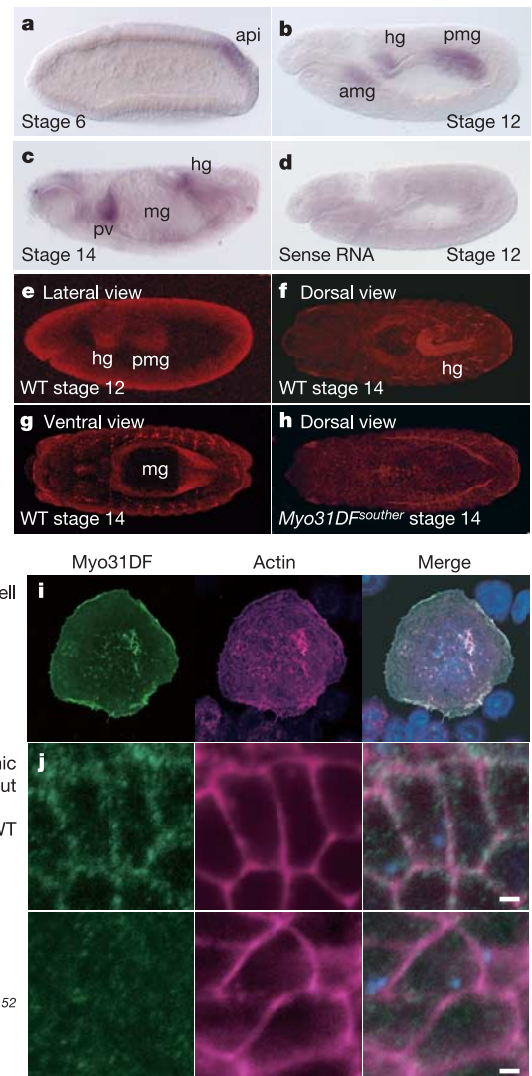


**Figure 2 | Embryonic expression of *Myo31DF* and the subcellular localization of *Myo31DF*.** **a–d**, *In situ* hybridization showing embryonic expression of *Myo31DF* at stage 6 (**a**), stage 12 (**b**) and stage 14 (**c**). **d**, Staining with a *Myo31DF* sense-strand RNA probe. **e–h**, *Myo31DF* detected with anti-Myo31DF-1P antibody in wild-type (**e–g**) and *Myo31DF*<sup>souther</sup> (**h**) embryos at stage 12 (**e**) and stage 14 (**f–h**). **i, j**, Localization of *Myo31DF* in S2 cells (**i**) and hindgut epithelial cells (**j**). *Myo31DF*-GFP (**i**, left) and endogenous *Myo31DF* (**j**, left) are green, actin (**i, j**, middle) is purple; toto3 nuclear staining is blue. Right panels show the merged images. Scale bar, 1 μm. Abbreviations: amg, anterior midgut primordium; api, amnioproctodeal invagination; hg, hindgut; mg, midgut; pmg, posterior midgut primordium; pv, proventriculus.

**Table 1 | Percentage of flies showing handedness defects**

Genotype	Embryonic phenotype					Adult phenotype			
	Foregut inverse	Foregut deformed	Midgut inverse	Hindgut inverse	Midgut and hindgut deformed	Hindgut inverse	Hindgut deformed	Testis inverse	Testis deformed
Wild-type	0.5(1/200)	2.5(5/200)	0.4(1/247)	0.4(1/247)	2.4(7/247)	0.0(0/55)	0.0(0/55)	0.0(0/56)	7.1(4/56)
<i>Myo31DF<sup>souther</sup></i>	0.0(0/51)	0.0(0/51)	75.7(28/37)	75.7(28/37)	5.4(2/37)	40.7(22/54)	29.6(16/54)	73.7(28/38)	18.4(7/38)
<i>Myo31DF<sup>L152</sup></i>	1.9(1/51)	0.0(0/51)	82.0(105/128)	82.0(105/128)	6.3(8/128)	85.7(30/35)	2.9(1/35)	78.7(37/47)	19.1(9/47)
<i>Myo31DF<sup>L152</sup> / Df(2L)J2</i>	-	-	57.7(30/52)	61.5(31/52)	6.0(3/52)	-	-	-	-
<i>UAS-gfp-moesin / byn-Gal4</i>	0.0(0/41)	0.0(0/41)	29.4(5/17)	47.5(28/59)	0.0(0/59)	-	-	-	-
<i>Myo31DF<sup>L152</sup>; UAS-gfp-moesin / byn-Gal4</i>	0.0(0/8)	0.0(0/8)	60.0(3/5)	52.8(19/36)	0.0(0/36)	-	-	-	-
<i>UAS-Rho N19 / NP2432</i>	-	-	28.9(22/76)	21.0(16/76)	9.2(7/76)	-	-	-	-
<i>UAS-Myo61F / byn-Gal4</i>	-	-	100.0(17/17)	100.0(36/36)	0.0(0/36)	-	-	-	-
<i>UAS-Myo31DF / byn-Gal4</i>	-	-	0.0(0/47)	0.0(0/47)	0.0(0/47)	-	-	-	-
<i>UAS-dsRNA Myo61F / P{Gal4-nos.NGT}40</i>	1.5(1/65)	0.0(0/65)	7.7(5/65)*	0.0(0/65)	1.5(1/65)	-	-	-	-
Rescue experiments ( <i>Myo31DF<sup>souther</sup></i> background)									
<i>UAS-Myo31DF / +</i>	-	-	46.3(37/80)	46.3(37/80)	2.5(2/80)	-	-	-	-
<i>UAS-Myo31DF / NP2432</i>	-	-	0.0(0/40)	0.0(0/40)	7.5(3/40)	-	-	-	-

The percentage of embryos showing defects in handedness (inverse) or deformation of organs (deformed) is shown. Genotypes of the examined embryos and adults are indicated on the left. Actual numbers of scored embryos and adults are shown in parentheses. -, values not determined.

\*Embryos showing partial inversion of midgut handedness are included.

function, given that its overexpression rescued *Myo31DF<sup>souther</sup>* (Supplementary Table 1, row 26). *Myo31DF*-GFP co-localized with actin, mostly at cell protrusions (Fig. 2i). In epithelial cells of the hindgut, endogenous *Myo31DF* was detected as punctate staining, partly overlapping with cortical actin (Fig. 2j).

*byn-Gal4*-driven misexpression of GFP-tagged moesin, an actin-binding protein, in wild-type embryos caused a reduction in actin filaments in the apical region of the hindgut epithelium, where *Myo31DF* function is required<sup>13</sup> (Fig. 3a,b). Notably, the midgut and hindgut always had the same handedness, but the handedness was random (not inverted), in wild-type and *Myo31DF* homozygous embryos (Table 1, rows 5 and 6). Embryo handedness was also affected by NP2432-driven GFP-moesin expressed in the hindgut epithelium only (Supplementary Table 1, row 12). However, GFP-moesin expression in the midgut only did not affect handedness (Supplementary Table 1, row 13).

To investigate further the functional link between *Myo31DF* and the actin cytoskeleton, we determined the phenocritical period for inducing left-right defects using *Myo31DF* RNAi and GFP-moesin misexpression, following the TARGET method<sup>14</sup>. Both *Myo31DF* knockdown and GFP-moesin expression in the hindgut 0–24 h after pupation caused similar defects in adult gut handedness, suggesting that *Myo31DF* and the appropriate organization of actin filaments are required at the same time (Supplementary Table 2). GFP-moesin also affected handedness in the *Myo31DF* embryo, suggesting that the default handedness, which may be manifested in the *Myo31DF* homozygote, also depends on the actin cytoskeleton (Table 1, row 6). We also examined the involvement of three Rho GTPase family proteins, Rho, Rac and Cdc42, which regulate the organization of the actin cytoskeleton<sup>15</sup>. Expression of dominant-negative forms of these proteins, especially Rho, in the hindgut induced synchronous left-right defects in the embryonic midgut and hindgut (Table 1, row 7 and Supplementary Table 1, rows 14 and 16). Together, our results suggest that *Myo31DF* depends on the actin cytoskeleton to generate left-right asymmetry.

Cell division and cell death do not occur during left-right asymmetric development of the hindgut<sup>16</sup>. We therefore speculated that the rearrangement of hindgut epithelial cells may be part of this

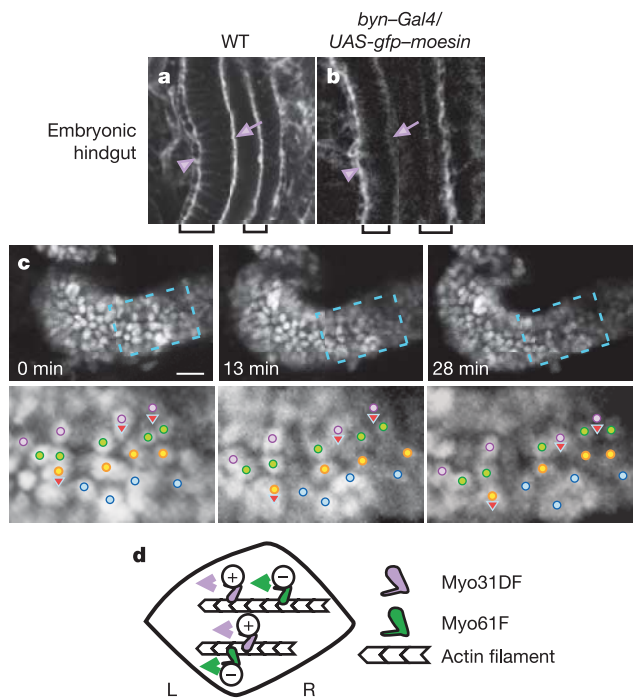


**Figure 3 | *Myo31DF* is dependent on the actin cytoskeleton to develop left-right asymmetry.** **a, b**, Actin localization in hindgut epithelium of wild-type (**a**) and GFP-moesin-overexpressing (**b**) embryos. The basal surface is indicated with an arrowhead, the apical surface with an arrow, and hindgut epithelial cell layers are indicated with brackets. **c**, Time-lapse analysis of hindgut epithelial cells. Dots of each colour indicate a single row of cells at  $t = 0$  min. Images obtained at 0, 13 and 28 min are shown. The lower panels show a higher magnification image of the boxed area in each upper panel. Note that each row of cells tilts (with right becoming upper), which coincides with the left-handed rotation of the hindgut. Cells showing intercalation are indicated with arrowheads showing the direction of their movement. Scale bar, 10  $\mu$ m. **d**, Model for myosin I protein functions in *Drosophila* left-right asymmetry. *Myo31DF* and *Myo61F* transport left-right determinants with opposite activities.

process. To test this possibility, we performed a time-lapse analysis. The position of each cell was visualized by labelling the nucleus with GFP. Cell rearrangement, which coincided with the left–right bias associated with left-handed rotation of the hindgut, was suggested by the significant intercalation of some cells (arrowheads in Fig. 3c).

Another myosin I protein, Myo61F (*Drosophila* MyoIB, also referred to as MyoIC in mammals), has been reported in *Drosophila*<sup>3,4,17</sup>. Myo61F protein is detected in the embryo and adult gut<sup>4</sup>. To test whether *Myo61F* is also involved in left–right asymmetry, we overexpressed *Myo61F* using *UAS-Myo61F* or GS9889 driven by *byn-Gal4* (Gene Search; Fig. 1b). Unexpectedly, Myo61F overexpression resulted in inversion of the midgut and hindgut in both cases (Table 1, row 8, and data not shown). In contrast, *Myo31DF* overexpression did not affect the handedness of these organs (Table 1, row 9). These results suggest that Myo31DF and Myo61F have antagonistic functions in creating the left–right asymmetry of these organs. The involvement of Myo61F in left–right asymmetry is also supported by our finding that its knockdown by RNAi results in the left–right defect in the embryonic midgut (Table 1, row 10).

We have found that homozygous *Myo31DF* embryos show reversed handedness of embryonic and adult visceral organs, which may represent the default state of left–right asymmetry in *Drosophila*. This situation is similar to the function of the *sinistral* gene in the freshwater snail, *Limnea* (although the *sinistral* gene is required maternally)<sup>1,18</sup>. Normal handedness is still seen in 25% of *Myo31DF* homozygotes. We speculate that some other myosin gene(s) has a redundant function in left–right patterning. Inversion of the anteroposterior axis does not affect laterality, suggesting that left–right patterning occurs zygotically<sup>7</sup>; this is consistent with the zygotic function of *Myo31DF*. Our results also suggest that an actin-based mechanism, which can align itself to either an anteroposterior–dorsoventral reference or the pre-existing sinistral handedness, exists to direct the rotation of the hindgut epithelium. As myosin I proteins are involved in vesicular transport<sup>19</sup>, we propose that Myo31DF and Myo61F, which on the basis of their structures are believed to move to the plus ends of actin filaments, carry left–right determinants with opposite activities (Fig. 3d). Thus, both left–right determinants would be concentrated in the plus ends of actin filaments that have a hypothetical planar polarity. In the *Myo31DF* mutant, only the opposing determinant is concentrated here, which reverses the handedness. According to our model, disruption in actin organization would result in left–right randomization, as we indeed observed experimentally.

## METHODS

***Drosophila* stocks.** We used Canton-S as the wild-type *Drosophila* strain. *Myo31DF<sup>souther</sup>* and *Myo31DF<sup>L152</sup>* are newly characterized *Myo31DF* mutations. GS9889 is a Gene Search line. *Df(2L)J2* has a deletion between 31B and 32A (Bloomington Stock Center). The following GAL4 drivers were used: *byn-Gal4* drives GAL4 expression in the hindgut and the posterior midgut primordium at stage 8, and in the longitudinal visceral mesoderm at stage 11 (ref. 11). *da-Gal4* drives uniform GAL4 expression<sup>12</sup>. *how<sup>24B</sup>* drives GAL4 expression in the mesoderm primordium from stage 11 (ref. 20). 48Y drives GAL4 expression in the anterior and posterior midgut primordium from stage 10 (ref. 21). NP2432 drives GAL4 expression in the hindgut epithelium from stage 9 (fly stock from National Institute of Genetics, <http://www.shigen.nig.ac.jp/fly/nigfly>; data not shown). NP5021 drives GAL4 expression in the whole gut from stage 9 (fly stock from National Institute of Genetics; data not shown). *P{Gal4-nos.NGT}40* expresses *Gal4* mRNA maternally<sup>22</sup>.

The following *UAS* lines were used: *UAS-gfp-moesin*, which encodes a fusion protein of the actin-binding domain of moesin and GFP (provided by S. Hayashi)<sup>13</sup>; *UAS-Rho N19* (ref. 23); *UAS-Rac1 N17* (ref. 24); *UAS-Cdc42 F89* (ref. 25); *UAS-Myo31DF* (provided by S. Noselli); *UAS-Myo31DF-GFP* and *UAS-2 × Myo31DF<sup>RNAi</sup>*. The last two *UAS* lines are described in the accompanying paper<sup>10</sup>.

*UAS-Myo61F* lines carry a pUAST transformation vector that has an insertion of the entire open reading frame of *Myo61F* cDNA (clone GH04201). *UAS-dsRNA Myo61F* lines carry a construct in which *Myo61F* cDNA corresponding to nucleotides 446–848 of GH04201 was inserted into pUAST as an inverted repeat

with an interruption of the *Myo61F* fourth intron. *UAS-dsRNA Myo61F* was maternally driven by *P{Gal4-nos.NGT}40*. The genotypes of each embryo were determined using appropriate blue-balancers, such as *CyO*, *P{en1}wg<sup>en11</sup>* and *TM3, ftz-lacZ*. All crosses, except those used for the TARGET analysis, were performed at 25 °C on standard *Drosophila* medium.

**Analysis of phenocritical periods.** We used the TARGET method to determine the phenocritical periods for inducing the left–right defect of the adult gut by knocking down *Myo31DF* and expressing of GFP–moesin<sup>14</sup>. We used a temperature-sensitive GAL80, a suppressor of GAL4, to control the activity of GAL4 driven by *byn-Gal4*. This allowed us to express a double-stranded RNA corresponding to a portion of *Myo31DF* mRNA and to express GFP–moesin in a temporally specific manner. Flies were cultured at 18 °C, and pupae were collected at 24-h intervals. Pupae collected 0–24, 24–48 and 48–72 hours after pupation were cultured at 30 °C until eclosion.

**Histological analyses of embryos.** Antibody staining of *Drosophila* embryos was performed as previously described<sup>26</sup>. Embryos were photographed using Zeiss Axioskop2 plus or Zeiss Pascal microscopes. Primary antibodies were a mouse anti-Fasciclin III antibody (7G10, Developmental Studies Hybridoma Bank; 1:100 dilution)<sup>27</sup> and a rabbit anti-Myo31DF-1P antibody (1:10 dilution). The anti-Myo31DF-1P rabbit serum was raised against a glutathione *S*-transferase fusion protein containing Myo31DF amino acids 728–990 (also described in ref. 10). The anti-Myo31DF-1P antibody was affinity purified using the same Myo31DF polypeptide with a His-tag. Secondary antibodies were Cy3 anti-rabbit IgG, Cy3 anti-mouse IgG, and anti-rabbit Alexa488 (Jackson ImmunoResearch; used at 1:1,000 dilution). Toto3 was used as a nuclear marker (Molecular Probes; 1:200 dilution). Actin filaments were stained with rhodamine–phalloidin<sup>28</sup> (Molecular Probes; 1:200 dilution). Whole-mount *in situ* hybridization was carried out as described<sup>29</sup>. A digoxigenin-labelled RNA probe was prepared from a full-length cDNA template of *Myo31DF* using a DIG RNA labelling kit (Roche).

**Microscopic analysis of embryonic gut handedness.** Genotypes of the embryos that were selected for study were identified by the lack of blue-balancers after  $\beta$ -galactosidase staining<sup>26</sup>. The handedness of the foregut, midgut and hindgut were scored at stages 15–16, stage 16, and stages 14–16, respectively.

**Cell culture and staining.** *Drosophila* S2 cells were plated and cultured on concanavalin A (Sigma) as previously described<sup>30</sup>. The cells were co-transfected with pUAS-*Myo31DF-GFP* and pAyGAL4 using CellFECTIN (Invitrogen). S2 cells were fixed and stained as described<sup>30</sup>. The secondary antibody used was anti-rabbit Alexa488 (Jackson ImmunoResearch; 1:200 dilution). Staining with rhodamine–phalloidin (1:40 dilution) was carried out as described<sup>28</sup>. The nuclear marker was toto3 (1:200 dilution).

**Time-lapse analysis.** Live embryos expressing NP5021-driven *UAS-GFP<sup>nl5</sup>* in the whole gut were mounted with FL-100 (Shin-Etsu Chemical Co.). Images were collected on a Zeiss Pascal microscope at intervals of 25 s from stage 13 onwards, and were processed with Zeiss LSM Image Browser and Adobe Photoshop software.

Received 20 September 2005; accepted 2 February 2006.

- Wood, W. B. Left–right asymmetry in animal development. *Annu. Rev. Cell Dev. Biol.* **13**, 53–82 (1997).
- Mercola, M. & Levin, M. Left–right asymmetry determination in vertebrates. *Annu. Rev. Cell Dev. Biol.* **17**, 779–805 (2001).
- Gillespie, P. G. et al. Myosin-I nomenclature. *J. Cell Biol.* **155**, 703–704 (2001).
- Morgan, N. S., Heintzelman, M. B. & Mooseker, M. S. Characterization of Myosin-IA and Myosin-IB, two unconventional myosins associated with the *Drosophila* brush border cytoskeleton. *Dev. Biol.* **172**, 51–71 (1995).
- Hayashi, T. & Murakami, R. Left–right asymmetry in *Drosophila melanogaster* gut development. *Dev. Growth Differ.* **43**, 239–246 (2001).
- Ligoxygakis, P., Strigini, M. & Averof, M. Specification of left–right asymmetry in the embryonic gut of *Drosophila*. *Development* **128**, 1171–1174 (2001).
- Hayashi, M. et al. Left–right asymmetry in the alimentary canal of the *Drosophila* embryo. *Dev. Growth Differ.* **47**, 457–460 (2005).
- Pascual, A., Huang, K., Neven, J. & Pr at, T. Neuroanatomy: Brain asymmetry and long-term memory. *Nature* **427**, 605–606 (2004).
- Adam, G., Perrimon, N. & Noselli, S. The retinoic-like juvenile hormone controls the looping of left–right asymmetric organs in *Drosophila*. *Development* **130**, 2397–2406 (2003).
- Sp der, P.,  ad m, G. & Noselli, S. Type ID unconventional myosin controls left–right asymmetry in *Drosophila*. *Nature* doi:10.1038/nature04623 (this issue).
- Iwaki, D. D. & Lengyel, J. A. A Delta–Notch signaling border regulated by Engrailed/Inverted repression specifies boundary cells in the *Drosophila* hindgut. *Mech. Dev.* **114**, 71–84 (2002).
- Wodarz, A., Hinz, U., Engelbert, M. & Knust, E. Expression of crumbs confers apical character on plasma membrane domains of ectodermal epithelia of *Drosophila*. *Cell* **82**, 67–76 (1995).

13. Edwards, K. A., Demsky, M., Montague, R. A., Weymouth, N. & Kiehart, D. P. GFP-moesin illuminates actin cytoskeleton dynamics in living tissue and demonstrates cell shape change during morphogenesis in *Drosophila*. *Dev. Biol.* **191**, 103–117 (1997).
14. McGuire, S. E. *et al.* Spatiotemporal rescue of memory dysfunction in *Drosophila*. *Science* **302**, 1765–1768 (2003).
15. Etienne-Manneville, S. & Hall, A. Rho GTPases in cell biology. *Nature* **420**, 629–635 (2002).
16. Iwaki, D. D., Johansen, K. A., Singer, J. B. & Lengyel, J. A. *drumstick*, *bowl*, and *lines* are required for patterning and cell rearrangement in the *Drosophila* embryonic hindgut. *Dev. Biol.* **240**, 611–626 (2001).
17. Gillespie, P. G., Wagner, M. C. & Hudspeth, A. J. Identification of a 120 kd hair-bundle myosin located near stereociliary tips. *Neuron* **11**, 581–594 (1993).
18. Shibasaki, Y., Shimizu, M. & Kuroda, R. Body handedness is directed by genetically determined cytoskeletal dynamics in the early embryo. *Curr. Biol.* **14**, 1462–1467 (2004).
19. Huber, L. A. *et al.* Both calmodulin and unconventional myosin Myr4 regulate membrane trafficking along the recycling pathway of MDCK cells. *Traffic* **1**, 494–503 (2000).
20. Brand, A. H. & Perrimon, N. Targeted gene expression as a means of altering cell fates and generating dominant phenotypes. *Development* **118**, 401–415 (1993).
21. Martin-Bermudo, M. D., Dunin-Borkowski, O. M. & Brown, N. B. Specificity of PS integrin function during embryogenesis resides in the  $\alpha$  subunit extracellular domain. *EMBO J.* **16**, 4184–4193 (1997).
22. Tracey, W. D. Jr, Ning, X., Klingler, M., Kramer, S. G. & Gergen, J. P. Quantitative analysis of gene function in the *Drosophila* embryo. *Genetics* **154**, 273–284 (2000).
23. Strutt, D. I., Weber, U. & Mlodzik, M. The role of RhoA in tissue polarity and Frizzled signaling. *Nature* **387**, 292–295 (1997).
24. Luo, L., Liao, Y. J., Jan, L. Y. & Jan, Y. N. Distinct morphogenetic functions of similar small GTPases: *Drosophila* Drac1 is involved in axonal outgrowth and myoblast fusion. *Genes Dev.* **8**, 1787–1802 (1994).
25. Eaton, S., Auvinen, P., Luo, L., Jan, Y. N. & Simons, K. CDC42 and Rac1 control different actin-dependent processes in the *Drosophila* wing epithelium. *J. Cell Biol.* **131**, 151–164 (1995).
26. Sullivan, W., Ashburner, M. & Hawley, R. S. *Drosophila Protocols* (Cold Spring Harbor Laboratory Press, New York, 2000).
27. Patel, N. H., Snow, P. M. & Goodman, C. S. Characterization and cloning of fasciclin III: a glycoprotein expressed on a subset of neurons and axon pathways in *Drosophila*. *Cell* **48**, 975–988 (1987).
28. Frydman, H. M. & Spradling, A. C. The receptor-like tyrosine phosphatase Lar is required for epithelial planar polarity and for axis determination within *Drosophila* ovarian follicles. *Development* **128**, 3209–3220 (2001).
29. Jiang, J., Kosman, D., Ip, Y. T. & Levine, M. The dorsal morphogen gradient regulates the mesoderm determinant twist in early *Drosophila* embryos. *Genes Dev.* **5**, 1881–1891 (1991).
30. Rogers, S. L., Rogers, G. C., Sharp, D. J. & Vale, R. D. *Drosophila* EB1 is important for proper assembly, dynamics, and positioning of the mitotic spindle. *J. Cell Biol.* **158**, 873–884 (2002).

**Supplementary Information** is linked to the online version of the paper at [www.nature.com/nature](http://www.nature.com/nature).

**Acknowledgements** We thank the Developmental Studies Hybridoma Bank at the University of Iowa, the Bloomington Stock Center, and the *Drosophila* Genetic Resource Center at the Kyoto Institute of Technology. We thank J. Lengyel for *byn-Gal4* and S. Hayashi for *UAS-gfp-moesin* transgenic strains. This work was supported by grants-in-aid from the Japanese Ministry of Education, Culture, Sports and Science.

**Author Contributions** Experimental work was performed by S.H., R.M., K.T., M.K., S.S., T.S., P.S. and T.A. Data analysis was by S.H., R.M., K.T. and K.M., and project planning was coordinated by S.N., R.M. and K.M.

**Author Information** Reprints and permissions information is available at [npg.nature.com/reprintsandpermissions](http://npg.nature.com/reprintsandpermissions). The authors declare no competing financial interests. Correspondence and requests for materials should be addressed to K.M. ([matsuno@rs.noda.tus.ac.jp](mailto:matsuno@rs.noda.tus.ac.jp)).